# Mesostructured *m*-Cresol Formaldehyde, Resorcinol Formaldehyde and *m*-Aminophenol Formaldehyde Composite Resins: Their Adsorption and Optical Properties

**Nandi Mahasweta[1]\*, Mondal John[2] and Bhaumik Asim[3]\***

1. Integrated Science Education and Research Centre, Siksha Bhavana, Visva-Bharati, Santiniketan, West Bengal 731 235, INDIA
2. Inorganic and Physical Chemistry Division, CSIR-Indian Institute of Chemical Technology (IICT), Uppal Road, Hyderabad-500 007, INDIA
3. Department of Materials Science, Indian Association for the Cultivation of Science, Jadavpur, Kolkata 700 032, INDIA
*mahasweta.nandi@visva-bharati.ac.in; msab@iacs.res.in

## Abstract

*Three mesostructured resol frameworks have been synthesized through condensation between m-cresol formaldehyde, resorcinol formaldehyde and m-aminophenol formaldehyde. The resol derived from m-cresol and resorcinol with formaldehyde have been synthesized using supramolecular assembly of cationic surfactant under alkaline pH conditions whereas for the preparation of m-aminophenol-formaldehyde composite, self-assembly of a neutral surfactant has been used under acidic pH condition. The resin of m-aminophenol and formaldehyde has been used as precursor for N-doped mesoporous carbon. All the materials have been characterized thoroughly using powder X-ray diffraction, transmission and scanning electron microscopy, nitrogen and hydrogen sorption studies, thermal analysis and UV-Vis and photoluminescence spectroscopy.*

*These composite materials exhibit photoluminescence property at room temperature. All the organic nano-composite materials after template extraction showed relatively low surface area. The carbon sample derived from m-aminophenol formaldehyde showed considerable surface area. The dye absorption property of the template extracted m-aminophenol formaldehyde composite and the mesoporous carbon material has been studied using some organic dyes. It has been found that the all organic composite is capable of efficiently adsorbing these dyes compared to the carbon aerogel. The adsorption is expected to proceed via strong interaction of the dye molecules with the reactive functional groups present in the resol framework.*

**Keywords:** Organic framework, Carbon, Mesoporous, Dye adsorption, Optical property.

## Introduction

Surfactant templating route for the synthesis of mesoporous materials utilizes supramolecular assembly[1] formed by surfactant molecules as core around which a solid inorganic matrix is formed. Subsequent removal of surfactant molecules from this composite generates meso-porosity based on the size of the self-assemblies in those solid materials. Since the first report of the synthesis of ordered mesoporous silica in 1992[2], this soft templating approach for the synthesis of ordered nanostructured materials has been extensively practiced.

Mesoporous materials invented so far utilizing this synthesis strategy have been used for adsorption, ion-exchange, catalysis and as hosts for nanomaterials synthesis as they have very high surface area and tuneable pore sizes compared to microporous materials.[3]

Beside silica based materials, other mesoporous frameworks have also found huge potential applications in catalysis,[4,5] adsorption,[6,7] electronics[8] and sensors.[9] However, only a few studies have appeared so far on the direct templated synthesis of ordered mesoporous polymers.[10-16] The choice of the polymer precursor is the key to the successful organization of the organic-organic mesostructures.[17]

Mesoporous polymers are mostly prepared by the EISA (evaporation induced self-assembly) technique, typically using ethanol as solvent. However, similar materials can also be prepared in basic aqueous media by a liquid crystal templating or cooperative assembly mechanism.[18] Most of the reported mesoporous polymers are phenol-formaldehyde (resol) resins mainly used as a precursor for mesoporous carbon. Few studies have appeared on other polymers like pyridine-phenol, polyaniline and polyacrylonitrile.[12,13,19]

A wide variety of ordered mesoporous polymer structures can be synthesized with different functional groups and pyrolysis of the meso-phase pitch and resins can generate carbon frameworks. N-doped porous carbons attracted special interest in this regard because it can simultaneously functionalize the carbon surface.[7,20] One way to achieve this target is to synthesize mesoporous polymers with high content of carbon.

Porous carbons are used as industrial adsorbents owing to their low cost, hydrophobic surface, high surface area and pore volumes, chemical inertness and good thermal and mechanical stability.[21] The application areas of these materials are wide and versatile including gas separation, water purification, catalysis, super capacitor and fuel cell,

high temperature insulation materials, etc.[22-28] When the adsorbents are polymers, dyes, vitamins or other large molecules, only mesopores allow adsorption of such molecules while commercial active carbons are by nature microporous. The preparation of mesoporous carbon materials with ordered open pore structures via a supramolecular templating approach is difficult due to the intrinsic characteristics of organic molecules and high formation energy of C–C bonds.

However, some interesting studies on the direct templated synthesis of mesoporous carbons have been reported.[14-18] This technique is more attractive than nano-casting approach using mesoporous ordered silica material as a hard-template and an organic precursor solution as the carbon source.[29-32] The process of producing mesoporous carbon using exo-casting is indirect and needs aggressive chemicals to remove the silica matrix. Major drawbacks associated with this method are the additional steps needed to prepare the silica backbones, sacrificial use of the silica host, high cost, extreme carbonization and dissolution conditions that affect the efficiency of the replication process. Thus, a direct soft templating approach via supramolecular assembly of surfactant for the synthesis of ordered mesoporous carbon is highly desirable.

Several research groups have developed various synthetic routes for the preparation of mesoporous carbons directly from organic-organic composites by supramolecular assembly of block copolymers as templates.[33-39] This approach employs the organic-organic interaction between a thermosetting polymer and a thermally decomposable surfactant to form a periodic ordered nanocomposite. The thermosetting polymer is carbonized by heating under nitrogen, leaving behind a carbonaceous pore wall. The pore sizes, wall thicknesses and pore symmetries of mesoporous materials thus obtained are predominantly determined by parameters of the structure directing agent (SDA) molecules, such as total molecular weight, hydrophilicity/ hydrophobicity ratio and volume fractions of the blocks of the templates.[39]

The selection of proper precursor is important. Resol with a large number of hydroxyl groups that strongly interacts with the triblock copolymer through the formation of hydrogen bonds is very interesting in this regard. Apart from phenol, resorcinol[37] or phloroglucinol[35] has also been used as building block to synthesize mesoporous polymeric matrices.

Triblock copolymer[14,15,39] templates have been used to synthesize ordered mesoporous polymers and carbon frameworks using phenol-formaldehyde resin as a carbon precursor via EISA method. The essence of these syntheses is to form a periodic meso-structure through hydrogen bonding interaction between resin and the hydroxyl groups (–OH) of triblock polymer. Upon pyrolysis, the porous

carbon structures are directly generated with the decomposition of the SDA.

In the present article, we shall discuss about the synthesis of mesostructured resol materials using supramolecular assembly of surfactant molecules as template followed by their hydrothermal treatment to produce the all-organic mesostructured composites. Removal of the template molecules by solvent extraction gives the all-organic porous materials. Three kinds of frameworks obtained from the condensation between *m*-cresol-formaldehyde, resorcinol-formaldehyde and *m*-aminophenol-formaldehyde will be discussed here.

Nanostructured resol samples derived from *m*-cresol and resorcinol with formaldehyde have been synthesized by using supramolecular assembly of a cationic surfactant through *in situ* aqueous polycondensation of *m*-cresol or resorcinol with formaldehyde at alkaline pH. For the preparation of *m*-aminophenol-formaldehyde composite, self-assembly of a neutral surfactant has been used under acidic pH condition. The resin derived from *m*-aminophenol and formaldehyde has been used as the precursor for the synthesis of an N-doped mesoporous carbon.[40]

The purely organic composites exhibit photoluminescence property at room temperature. The dye adsorption property of the template-free all-organic *m*-aminophenol-formaldehyde composite and mesoporous carbon material has been studied using some organic dyes. It is found that the all-organic composite is capable of efficiently adsorbing these dyes compared to the carbon aerogel. Such efficient adsorption is expected to proceed *via* strong interaction of the dye molecules with the functional groups present in the resol framework.

## Material and Methods
**Synthesis of nanostructured *m*-cresol formaldehyde and resorcinol formaldehyde composite resin:** Cationic surfactant cetyltrimethylammonium bromide (CTAB) was used as the structure directing agent. Organic precursor gels were synthesized via polycondensation of *m*-cresol/ resorcinol with formaldehyde (HCHO) in an aqueous alkaline solution of sodium hydroxide (NaOH). In a general synthetic procedure, 0.01 mole of CTAB was first dissolved in 20 ml of water. To it 0.04 mole of NaOH dissolved in 10 ml of water was added under stirring.

When the mixture becomes homogeneous, 0.04 mole of HCHO was added to it. Finally, 0.02 mole of *m*-cresol/resorcinol was added dropwise under constant vigorous stirring. After stirring for 2 h at room temperature, the gel was transferred into an airtight polypropylene bottle and kept at 363 K for 3 days. In a similar way, *m*-cresol/resorcinol formaldehyde resin was prepared without the assistance of any surfactant to obtain the non-porous material.

The solid products were then obtained through filtration, repeated washing with water and drying under vacuum. These as-synthesized samples of *m*-cresol formaldehyde and resorcinol formaldehyde have been designated as samples 1 and 2 respectively. Surfactant was removed from the as-synthesized samples by extracting two times with HCl/water for 4 h at room temperature. When the as-synthesized samples were extracted, it showed a considerable amount of weight-loss, *ca*. 50% which could be attributed to the loss of the surfactant molecules from the pores of the nanostructured as-synthesized mesostructured composites. The extracted samples of *m*-cresol formaldehyde and resorcinol formaldehyde are designated as samples 1a and 2a respectively.

**Synthesis of mesoporous *m*-aminophenol formaldehyde resin and its carbon:** In this synthesis neutral surfactant, Brij 56 was used as the structure directing agent. Organic precursor gels were synthesized via polycondensation of *m*-aminophenol with HCHO in an aqueous HCl solution. In a typical synthesis, 1.5 g of Brij 56 was first dissolved in 20 ml of water followed by the addition of 1.22 g of HCl. To it, 0.01 mole of *m*-aminophenol was added and dissolved under magnetic stirring at room temperature. Subsequently, 0.02 mole of HCHO was added to the above solution. The solution started becoming cloudy after about 15 min. The solution was stirred at room temperature for additional two hours till a dark yellow colored solid precipitated out completely from the synthesis gel.

The resulting solution was aged at 278 K overnight under static condition. The solid product was obtained through filtration, repeated washing with water and drying under vacuum in a lypholyzer. This material, designated as sample 3, has been used as a precursor to produce mesoporous carbon matrix. The powder was further cured at 373 K overnight before carbonization of the sample. It was then carbonized in a tubular furnace under nitrogen atmosphere via heating ramps of 1 K/min from 373 to 673 K and 5 K/min from 673 to 1123 K and it was kept at 1123 K for 2 h. Then the sample was gradually cooled to room temperature to get the carbonized material which has been named as 3a. The as-synthesized sample, 3, was extracted in water/ammonium acetate mixture to remove the template molecules and this sample has been designated as 3b.

## Results and Discussion

**X-ray powder diffraction:** Powder X-ray diffraction (PXRD) is one of the basic techniques to characterize nano-porous and nanostructured materials. PXRD patterns collected at low angles are important for the characterization of nano-porous materials and have an understanding of the size as well as ordering of the pores. In fig. 1(a-e), the low angle XRD patterns of the as-synthesized and extracted samples of *m*-cresol formaldehyde and resorcinol formaldehyde along with the non-templated *m*-cresol formaldehyde sample are shown.

A single low angle peak was observed for both the as-synthesized (fig. 1a and 1c) and extracted (fig. 1b and 1d) samples with no detectable peak at high angle indicating that the samples are nanostructured containing disordered meso-phases but there were no short or long range ordering. The extracted samples showed relatively weaker intensity and broader peak (fig. 1b and 1d) over the as-synthesized ones (fig. 1a and 1c). This result suggested that the nanostructure has been restored after the removal of the surfactant. However, the arrangement of the pores became more disordered after the removal of SDA.

The XRD pattern of the non-templated *m*-cresol formaldehyde sample (fig. 1e) showed no peak in the small angle region which confirms that the peak position obtained for the as-synthesized and extracted samples in no way reflects the size of resin particles merely, rather indicates the existence of meso-phase in the samples.

In fig. 1f and g, the small angle XRD patterns of the as-synthesized and carbonized samples of *m*-aminophenol-formaldehyde respectively are shown. A single intense small angle peak was observed for both the samples with no detectable peak at high angle indicating that the samples are mesoporous having disordered meso-phase but there are no short or long-range ordering. The carbonized sample showed relatively weaker intensity and broader peak width (Fig. 1f) over the as-synthesized one (Fig. 1g). Moreover, the position of the peak for the carbonized sample has been shifted to a higher value of 2θ. This result suggested that the nanostructure has been restored after carbonization but there is considerable amount of shrinkage in the size of the pores during the rigorous heating during carbonization.

**Electron microscopic studies:** Electron microscopic studies are often used to characterize the nanostructure and morphology of mesostructured materials. The transmission electron microscopic (TEM) images of samples 1 and 2 are shown in fig. 2. Fig. 2a and 2b depict the images for sample 1 whereas in fig. 2c the TEM image of sample 2 is shown. The images for both the samples confirm the formation of low electron density spherical spots of 2.0-2.5 nm diameter corresponding to small to medium size mesopores and their disordered arrangements. From fig. 2b, it is clear that sample 1 has cylindrical porous rod-like morphology. Interestingly, these nanosized rods are 150-300 nm long and 30-50 nm wide having pores of *ca*. 2.5 nm extended in all directions.

The transmission electron microscopic image of the carbonized sample 3a is shown in fig. 3a. The image confirms the formation of low electron density spherical spots of 2.5-3.0 nm diameters corresponding to the small to medium size mesopores and their disordered arrangements. Thus, from the PXRD and TEM analyses, it can be concluded that these mesostructured resol materials and the carbon derived from them have disordered wormhole-like nanostructure. In fig. 3b, the scanning electron microscopic (SEM) image of the carbonized sample 3a has been

displayed. The image clearly depicts the formation of particles with spherical morphology having diameters around 12-15 nm.

**Nitrogen adsorption/desorption studies:** Nitrogen sorption experiments at 77 K have been carried out to estimate the surface area and pore size of the samples. The nitrogen adsorption/desorption isotherms for samples 1a and 2a (not shown here) showed no sharp increase for $N_2$ uptake corresponding to the capillary condensation in the mesopore region. The estimated Brunauer-Emmett-Teller (BET) surface areas were 5.6 $m^2g^{-1}$ and 4.9 $m^2g^{-1}$ for samples 1a and 2a respectively. The pore size distribution of both the samples estimated by using Barett-Joyner-Halenda (BJH) method suggested a broad distribution with maxima at 2.5 nm and 2.3 nm respectively.

The isotherm for the *m*-cresol formaldehyde nanocomposite has been illustrated in fig. 4a along with the corresponding pore size distribution profile estimated by using BJH method in the inset. Since the framework of this porous resin

composites is completely organic containing aromatic fragments, bond twisting or bond distortion might have occurred leading to lower surface area in this material. Since, the resin surface is highly hydrophilic, removal of water molecules during degassing may result in collapse of the meso-structure in this case. Porous carbon synthesized from phenol and formaldehyde also exhibited similar low BET surface area (*ca.* 5 $m^2g^{-1}$).[35]

In fig. 4b, $N_2$ adsorption/desorption isotherms for the carbonized sample 3a derived from *m*-aminophenol and formaldehyde condensation have been illustrated. A typical type IV isotherm with a steep rise due to capillary condensation at relative pressure range 0.3-0.4, characteristic of mesoporous materials can be clearly seen.[33-35] The BET surface area for the sample is found to be 260 $m^2g^{-1}$. Pore size distribution profile of the sample using BJH model is given in the inset. A quite narrow distribution of pores with maxima at 2.7 nm is seen. Pore volume for this mesoporous carbon material is 0.2 cc $g^{-1}$.
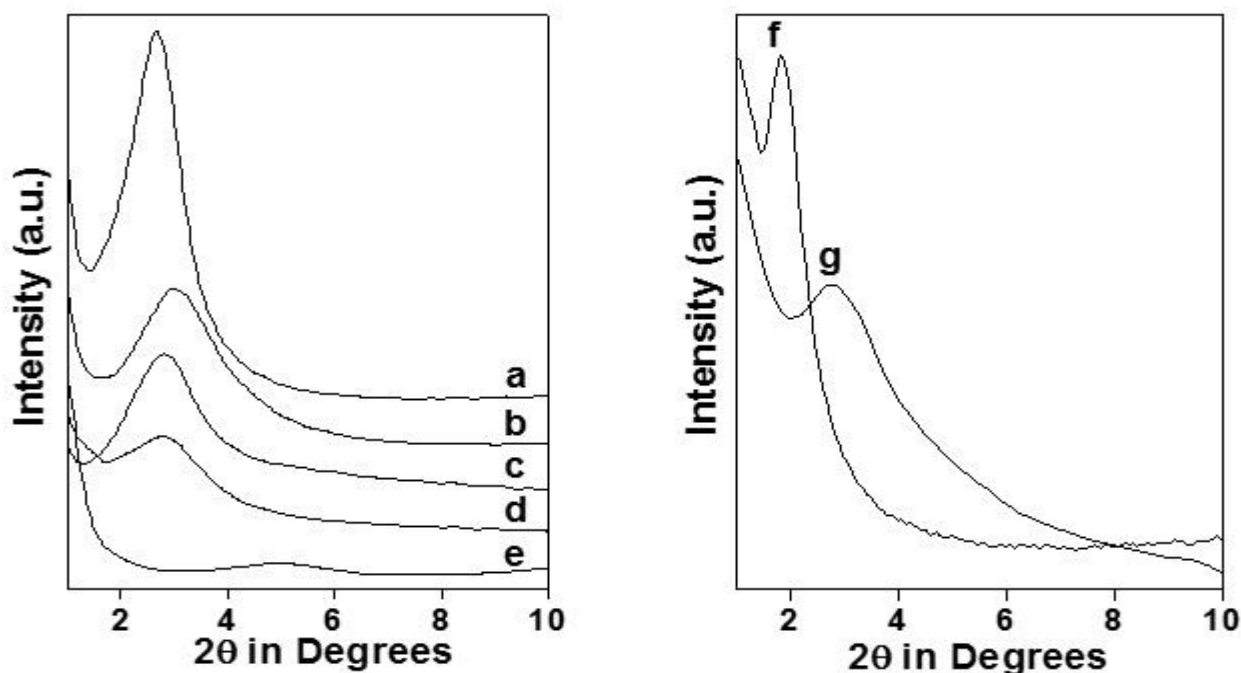


**Fig. 1: Small angle XRD pattern of 1 and 2 (a and c), 1a and 2a, (b and d), non-templated sample of m-cresol formaldehyde (e) and 3 and 3a (f and g)**
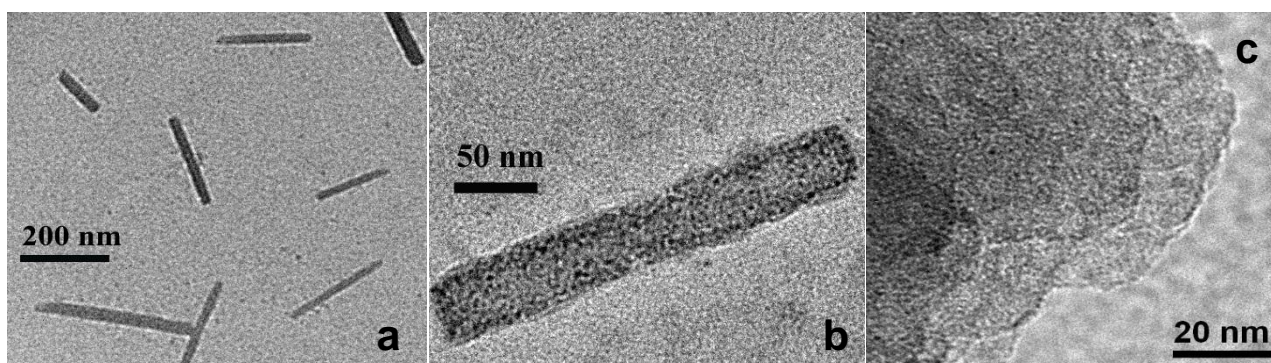


**Fig. 2: TEM image of as-synthesized samples of 1 (a and b) and 2 (c)**
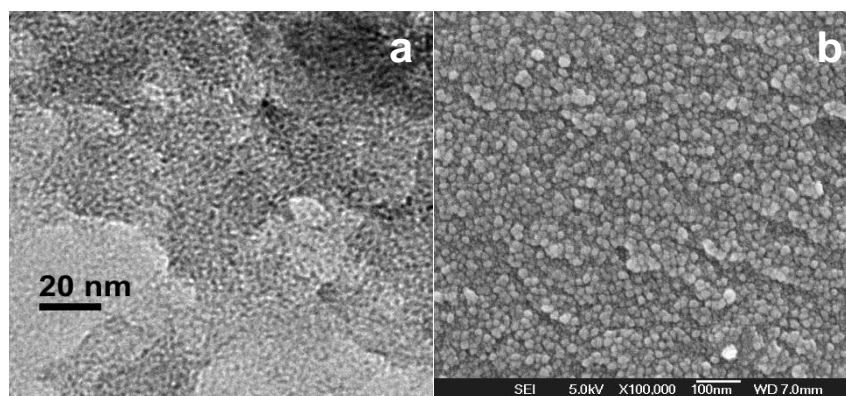
33

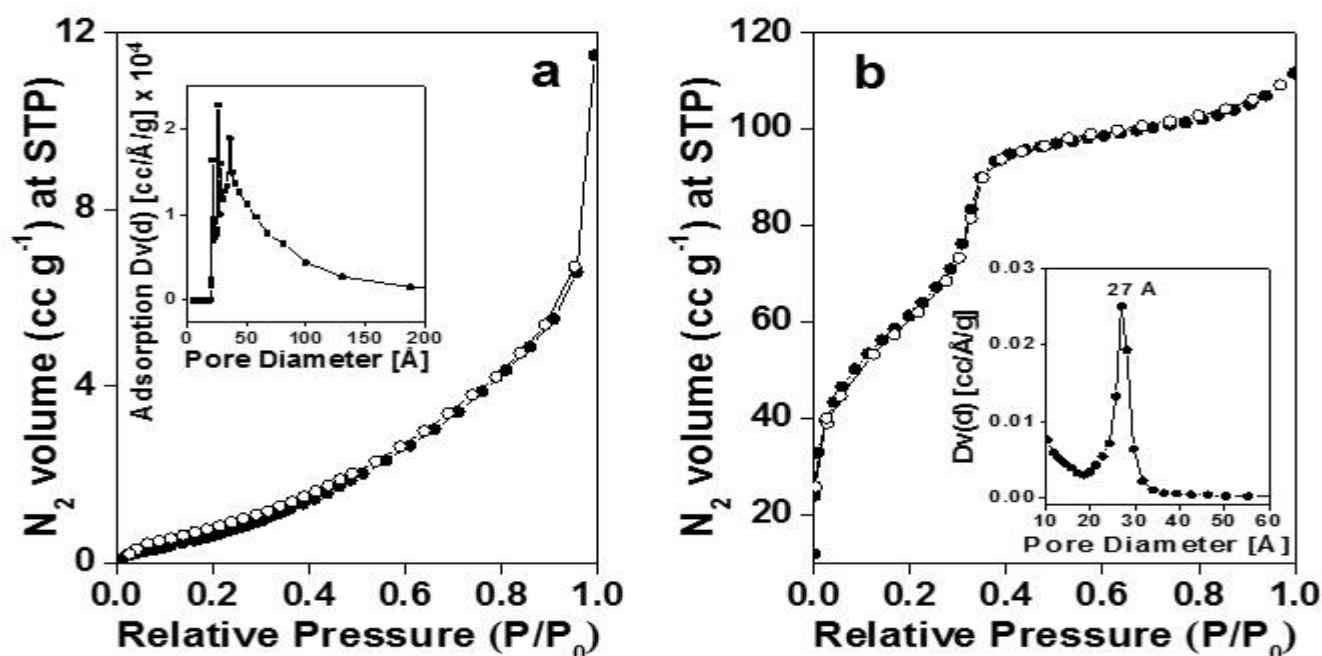**Fig. 3: (a) TEM and (b) SEM image of carbonized sample**



**Fig. 4: Nitrogen adsorption/desorption isotherms of (a) 1a and (b) carbonized sample 3a at 77 K.**
**Pore size distribution using BJH method is shown in the insets.**

**Thermogravimetry and differential thermal analysis:**
The quantitative determination of the content of *m*-cresol formaldehyde and resorcinol formaldehyde in the surfactant free samples 1a and 2a has been estimated by using thermogravimetry (TG) and differential thermal analysis (DTA) in the presence of $N_2$ flow. The TG and DTA plots of both the samples were found to have followed a similar trend and the profile for *m*-cresol formaldehyde sample has been illustrated in fig. 5a. Both the samples show the first weight loss up to 373 K due to desorption of physiosorbed water (about 3.2 wt % for *m*-cresol and 3.3 wt % for resorcinol). This is followed by a sharp decrease in the weight at temperatures between 473 and 573 K which could be attributed to the loss of resin fragments present in the matrices.

A considerable endothermic peak in the DTA plot centered at 553 K suggested that most of the resin fragment was

decomposed at this point. The total weight loss for the sample was *ca*. 30 wt% in the temperature range 473-573 K. However, from 573-873 K, a gradual weight loss of *ca*. 25 wt% occurred with an exothermic peak near 723 K which could be due to the complete conversion of the material into carbon.

Fig. 5b illustrates the TG-DTA plots of sample **3** derived from *m*-aminophenol, HCHO and Brij 56, under $N_2$ flow. This profile can help us understand the course of the decomposition process taking place during carbonization. As seen from the profile, up to 413 K the material is more or less stable and loses a very little of its weight (*ca.* 3.2%). After that up to 723 K, the sample loses drastically further *ca.* 50% of its weight. A sharp endotherm followed by wide and broad exotherm is associated with this weight loss. This can be attributed to further combustion followed by burning of the template alkyl polyether. After this point as the

temperature is increased, the sample steadily loses its weight and the residue is the carbonaceous material alone and the total weight of the carbon matrix left is only 21% of the total weight. Chemical analysis results suggested that the N-content in this mesoporous carbon is 5.4 wt % which is also in close agreement with other N-doped porous carbons synthesized by nano-casting method.[33]

Attempts to prepare mesoporous carbons using *m*-aminophenol and formaldehyde, using CTAB and sodium

dodecyl sulphate (SDS) resulted in collapse of the meso-phases during carbonization probably due to the ionic interactions between the resin framework and the ionic surfactants whereas for mesoporous carbon synthesized by using Brij 56 as template, there exists extremely weak H-bonding interaction between organic polymer frameworks and amphiphilic surfactants. This causes the reduction of interaction between organic frameworks and surfactants after polymerization and consequent macroscopic phase separation.[15]
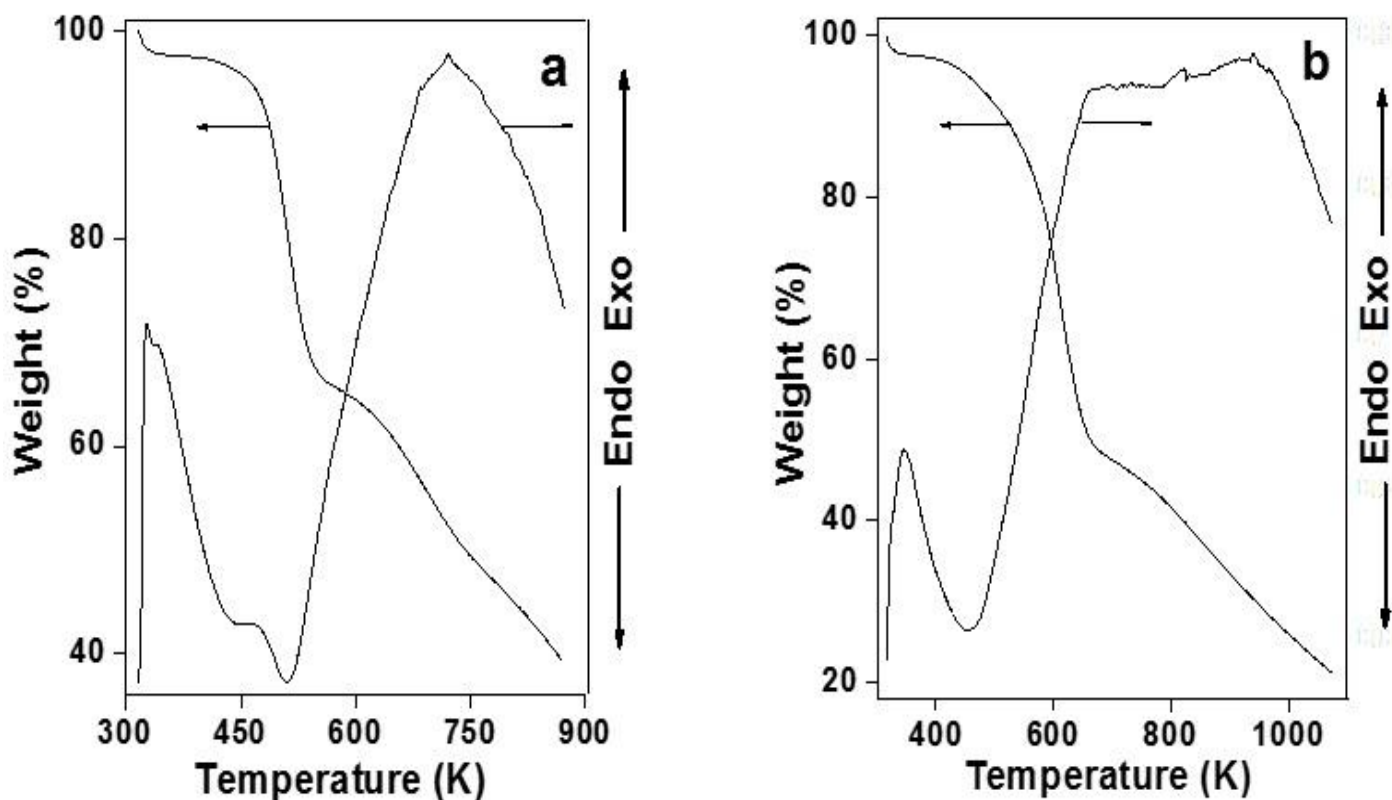


**Fig. 5: TG and DTA plots for sample 1a and 3**

**UV-Visible spectroscopy:** UV-visible diffuse reflectance spectra have been used to characterize the organic frameworks. In fig. 6, the UV-visible spectra for *m*-cresol-CHO samples and *m*-cresol dissolved in NaOH solution have been shown. Strong absorption bands at *ca.* 210, 240 and 290 nm for *m*-cresol/NaOH solution were observed (Fig. 6d) due to $\pi \rightarrow \pi^*$ transitions of different chromophoric functionalities whereas the as-synthesized and extracted samples, 1 and 1a (fig. 6a and b respectively), showed no absorption in this region; broad bands were observed at higher wavelengths of 300-450 nm and shoulder at nearly 550-650 nm.

Similar trend in the absorbance pattern was observed in case of the non-templated sample (fig. 6c). A close comparison between the UV-visible spectra for the as-synthesized and extracted samples with the non-templated *m*-cresol-HCHO composite sample suggests that the framework is same as that of nonporous *m*-cresol HCHO resin.

For resorcinol, strong absorption band at *ca.* 278 nm with a weaker one at 225 nm and two shoulders at 325 and 490 nm were observed (fig. 6g) attributed to the chromophoric functionalities in the molecule whereas the as-synthesized and extracted samples, 2 and 2a (fig. 7 e and f) showed no absorption near 278 nm, rather a broad band was observed at higher wavelengths around 325 and 375 nm respectively. The hump at 490 nm that can be observed for resorcinol is somewhat shifted to higher wavelength at 527 and 525 nm respectively for the as-synthesized and extracted samples. Absence of any absorption band from 210-290 nm for the as-synthesized and extracted samples of both 1 and 2 suggested that all the *m*-cresol or resorcinol moieties are fully polycondensed with HCHO in these materials.

**Photoluminescence spectroscopy:** In fig. 7, the photoluminescence spectra of samples 1 and 2 are given. For the as-synthesized sample 1, in the excitation spectra (fig. 7a), a peak at 398 nm was seen and on excitation at this

wavelength two emission peaks (fig. 7a'), one at 470 nm (low intensity) and another very broad at 542 nm (strong) were obtained. On the other hand, for the excitation spectra (fig. 7b) of the extracted sample, a noticeable hump at 380 nm and a distinct peak at 398 nm can be seen. Emission spectra for both the excitation wavelengths were recorded and in each case, similar kind of emission spectra was observed, hence the spectra for excitation at 398 nm are shown in fig. 7b'. In this case also an intense sharp peak at 470 nm and a broad peak at 542 nm were observed. The observed broadness in the peak at 542 nm for both the samples may be ascribed to the nanorod morphology and its size distribution.[41]

For sample 2, the emission spectrum of the as-synthesized sample (fig. 7d') was obtained by excitation (fig. 7d) of the polymer at the maximum absorption wavelength ($\lambda_{ex}$= 349 nm). The maxima in the emission spectra were observed at 468 nm (weak intensity) and 565 nm (strong intensity) which corresponded to deep blue and greenish light respectively. The existence of some small peaks around 470 nm regions could be attributed to the morphology and particle size distribution of the sample.[42]

Thus, upon irradiation, the materials excite an electron from the HOMO to the LUMO to generate the singlet excited state and subsequently the excited polymer resins relax to the ground state with the emission of green and yellow light. Neither *m*-cresol nor resorcinol or HCHO displayed any luminescence in the liquid state at room temperature. The presence of the resin frameworks may tighten the entire skeleton resulting in much weaker vibrations and more relaxation[43] which could be responsible for such photoluminescence.

The photoluminescence spectrum for the non-templated *m*-cresol HCHO sample has also been recorded. Interestingly, these resol particles did not show any distinct peak near 380 nm or 398 nm in the excitation spectra (fig. 7c); rather a small hump was noticed at 398 nm. On excitation at 398 nm, again two peaks were observed (fig. 7c'), the one at 470 nm remained unchanged but the second broad peak at 542 nm disappeared this time with the emergence of another peak at somewhat lower wavelength, 500 nm. Thus, it is seen that with the introduction of meso-phase/nanostructures in the *m*-cresol HCHO composite, the photoluminescence spectra change distinctly which is also applicable for the material derived from resorcinol. When we go from the non-templated resol to the meso-structured material, a considerable red shift is observed.

**Dye adsorption property:** The dye adsorption capacity of the carbonized and the template extracted samples of *m*-amino-phenol-HCHO, 3a and 3b has been studied for three organic dyes, namely, Rose Bengal, Methylene blue and Fluorescein. It is found that the template extracted all-organic polymer, 3b can efficiently adsorb Rose Bengal dye compared to the carbonized sample 3a. UV-visible spectroscopic study has been carried out for these samples.

In fig. 8a, the UV-visible spectra of Rose Bengal dye dissolved in water have been shown. When this solution is stirred with 3a for 4 h and filtered, the filtrate showed almost no change in the absorption intensity.

In a similar way, when the template extracted sample 3b is stirred with dye solution for 4 h and the absorption of the filtrate solution was measured, there is a drastic reduction in the absorption intensities of the various characteristic peaks for Rose Bengal dye. Thus, it can be said that the organic resol framework with amino groups can efficiently adsorb the dye molecules compared to the carbon material.

In a similar way, aqueous solutions of methylene blue and fluorescein were also stirred with 3a and 3b. In this case none of the samples was found to adsorb dye molecules. Thus, we can say that 3b selectively adsorbs Rose Bengal dye whereas the carbon material almost does not interact with these dye molecules. Moreover, to study the efficiency of dye exchange of the amino-resol, 3b, we have treated it in a mixture of three dyes in water. The UV-visible spectra of the mixture of dye in water and the filtrate after stirring for 4 h with 3b, have been shown in fig. 8b. The primary characteristic peak for the three dyes has been marked in the figure. As we see, the peak for Rose Bengal dye almost vanishes after the exchange procedure whereas the absorption peaks for methylene blue and fluorescein has been retained. Thus, we can conclude that 3b can efficiently and selectively adsorb Rose Bengal dye from a mixture of different dye solutions.

**Mechanism of meso-phase formation:** In fig. 9, a reaction scheme for the formation of mesoporous *m*-cresol/resorcinol-HCHO framework has been proposed, constructed on the basis of sol-gel framework structures formed when *m*-cresol/resorcinol condenses with HCHO in the presence of an acid or a base.[44,45] Here the condensation can take place randomly in all direction of the activated aromatic ring, giving rise to a cross-linked resin framework. The cationic polar head groups of the supramolecular assembly of the cationic surfactant can interact with phenoxide anions under alkaline pH conditions leading to the nanostructured material (II).

In fig. 10, the templating mechanism for the formation of meso-phase in case of *m*-aminophenol-HCHO condensation has been depicted. Here the interaction between the organic polymer frameworks and amphiphilic surfactants is through very weak hydrogen bonds which break during carbonization leaving the resin framework unperturbed. On the other hand, strong ionic interactions of CTAB/SDS with the resin framework could be the possible reason for the collapse of the meso-structure during carbonization. During carbonization, since H and O atoms disappear along with aromatic features and all framework carbon atoms become tetrahedrally coordinated with other four carbon atoms, mesopores get stable in 3D arrangements. This may cause high surface area of the mesoporous carbon material over the mesoporous resin.
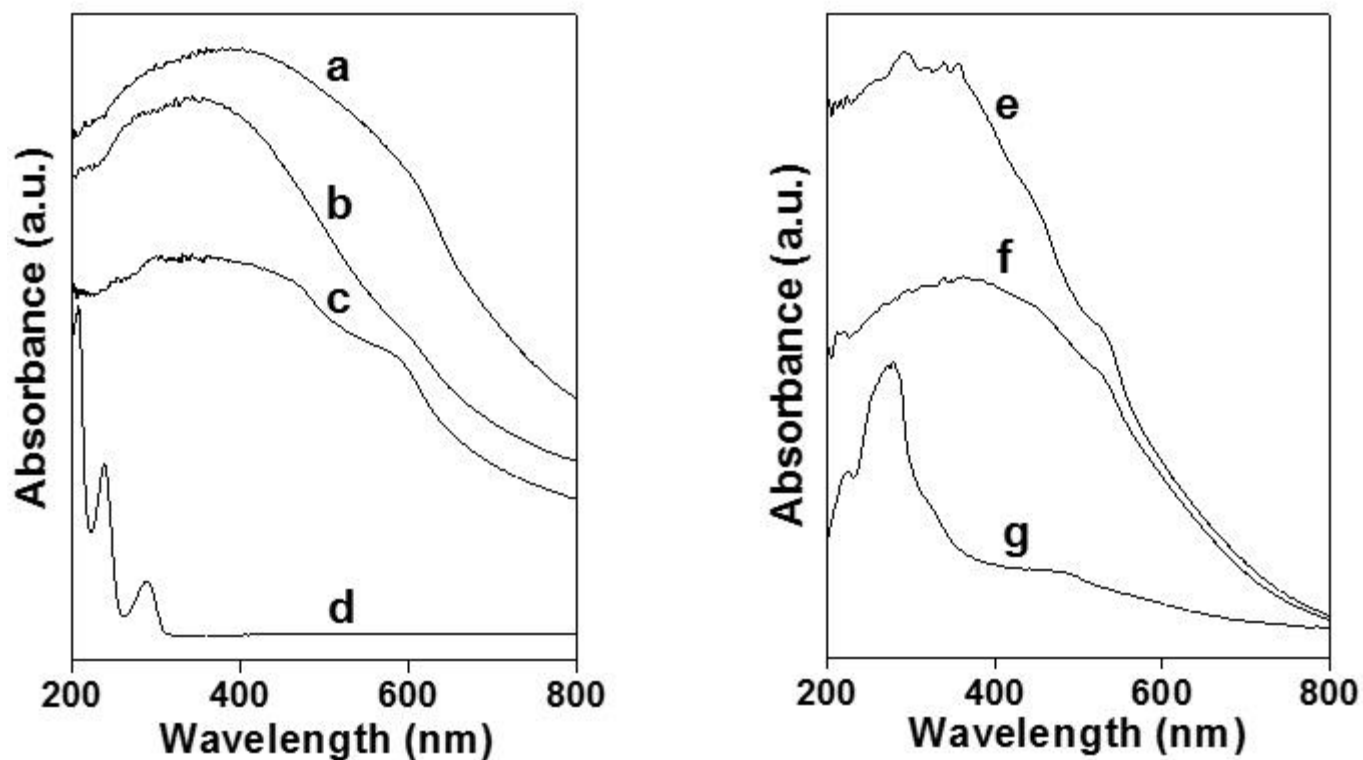
**Fig. 6: UV-Visible diffuse reflectance spectra of 1 (a) and 1a (b), non-templated *m*-cresol-formaldehyde (c) sample, m-cresol in NaOH solution (d), 2 (e) and 2a (f) and resorcinol in NaOH solution (g)**
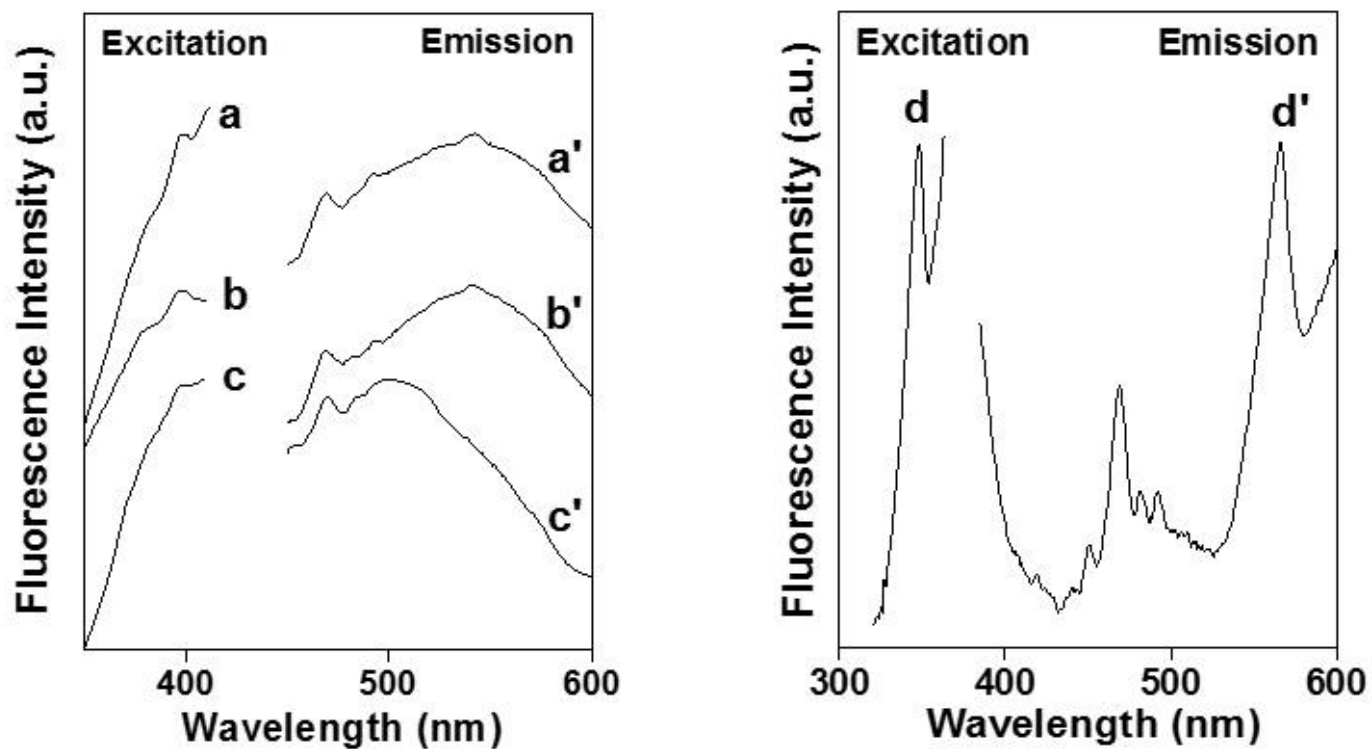


**Fig. 7: Photoluminescence spectra of 1: excitation (a) and emission (a'), 1a: excitation (b) and emission (b'), non-templated *m*-cresol-HCHO: excitation (c) and emission (c') and 2: excitation (d) and emission (d')**
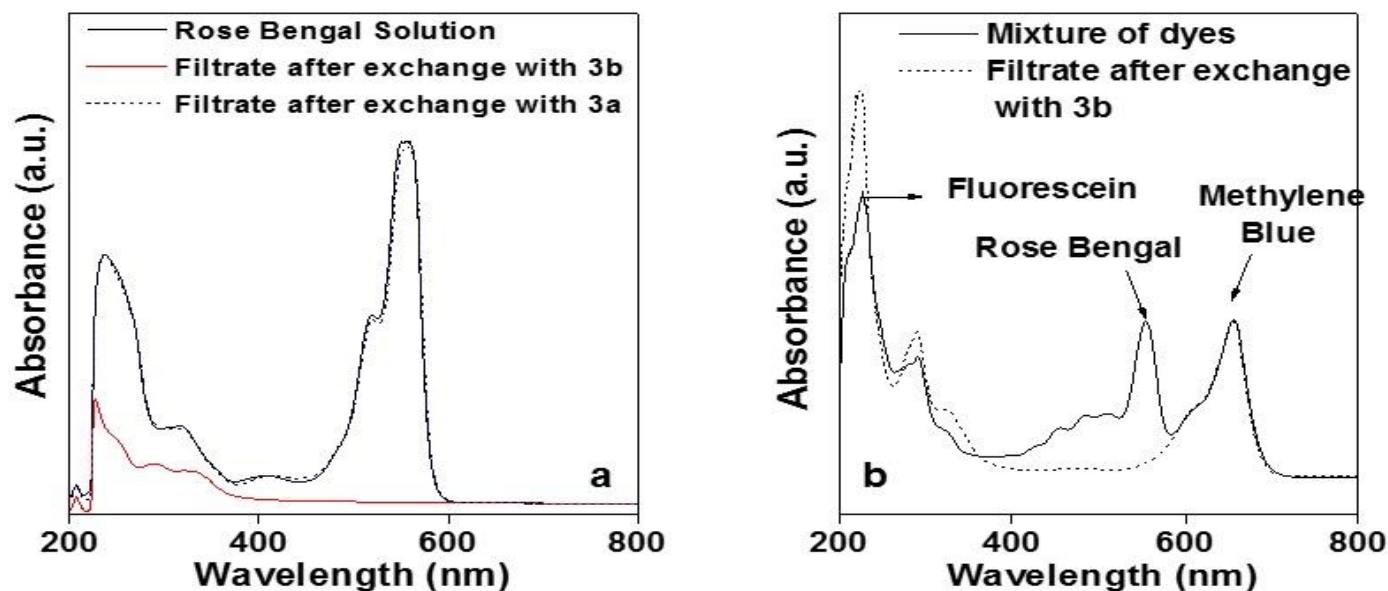
**Fig. 8: UV-visible spectra of (a) Rose Bengal dye before and after exchange with 3b and (b) mixture of dyes, before and after exchange with 3a and 3b**
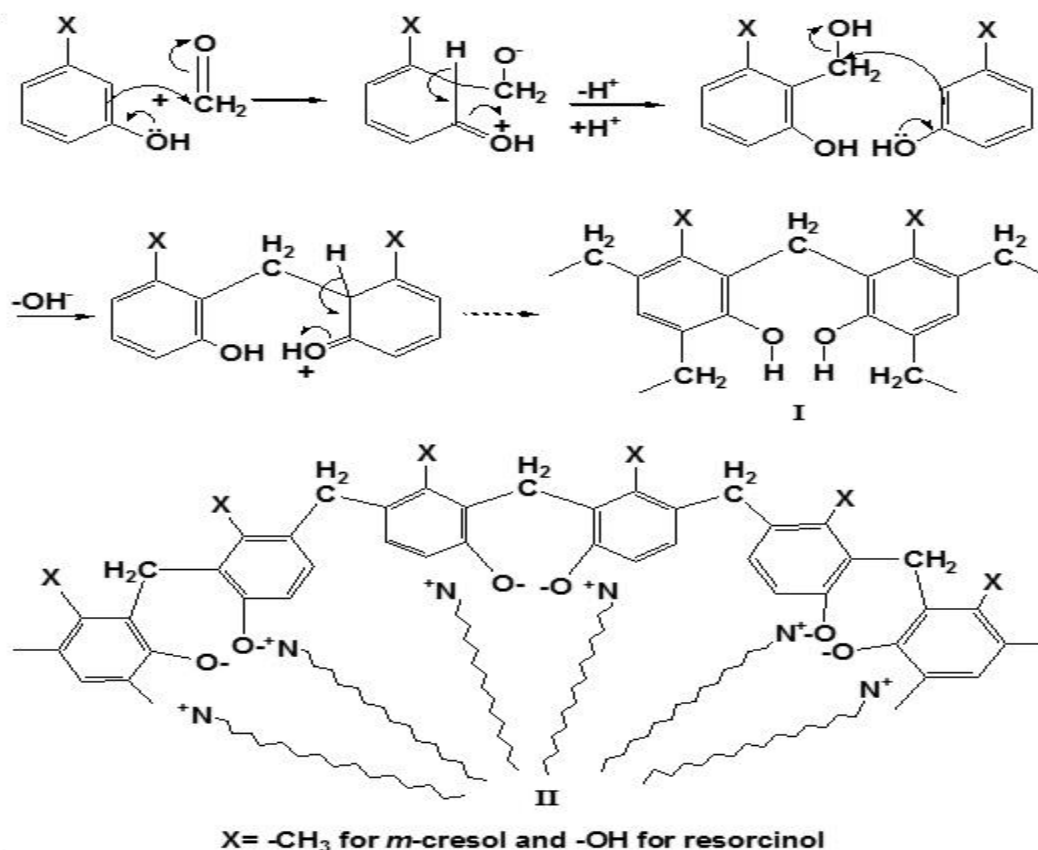


X= -CH₃ for *m*-cresol and -OH for resorcinol

**Fig. 9: Reaction scheme and proposed model (partial) for the formation of the nanostructures**

## Conclusion

In conclusion it can be said that nanostructured *m*-cresol/resorcinol-HCHO composites have been synthesized by using supramolecular assembly of a cationic surfactant CTAB through *in situ* aqueous polycondensation of *m*-cresol/resorcinol with HCHO in alkaline pH. Powder XRD and TEM studies suggested no short-range ordering in these samples and wormhole like disordered mesopores of dimension 2.3-2.5 nm extending in all direction. TEM image analysis suggested rod-like particles having dimensions of 150-300 nm in length and 30-50 nm in diameter for the *m*-cresol sample. UV-visible absorption data suggested the formation of polymeric resin network in these samples.

These composite materials exhibit photoluminescence property at room temperature. On the other hand, mesoporous carbon has been prepared using *m*-aminophenol-HCHO composite resin as the carbon

precursor under acidic pH condition using supramolecular assembly of a neutral surfactant Brij 56 as the structure directing agent. PXRD and TEM studies suggested no short-range ordering in this sample and wormhole like disordered mesopores with a pore size *ca.* 2.7 nm. SEM images taken for the sample showed almost uniform spherical particles of 15-18 nm distributed homogeneously. Nitrogen sorption studies suggested type IV isotherm with pore diameter of *ca.* 2.7 nm and a BET surface area *ca.* 260 $m^2g^{-1}$ for the carbon

sample. The mesoporous organic composite efficiently and selectively adsorbs Rose Bengal dye from a mixture of different dye molecules.

## Acknowledgement
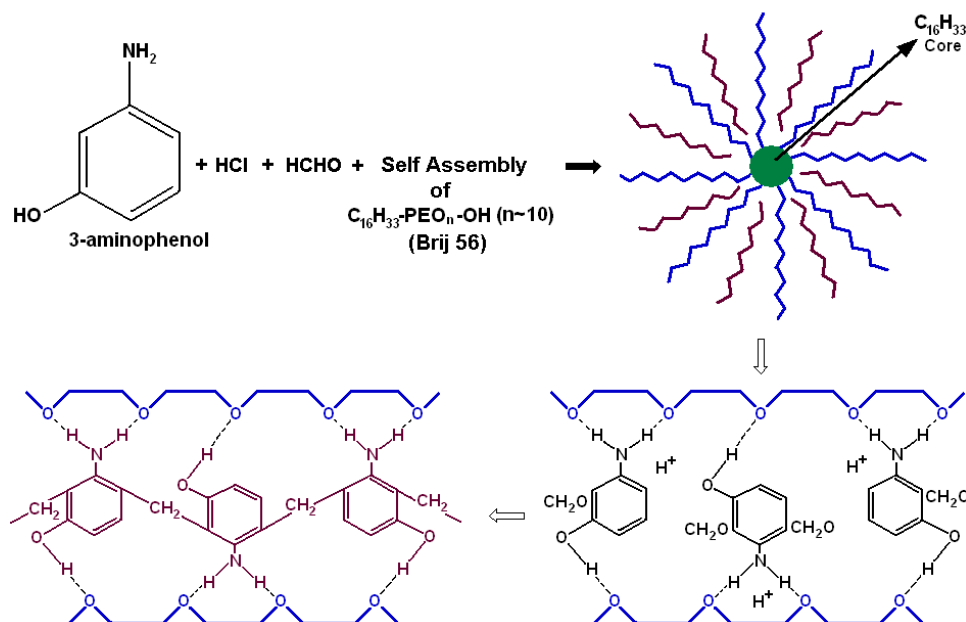
## References

1. Firouzi A., Atef F., Oertli A.G., Stucky G.D. and Chmelka B.F., Alkaline Lyotropic Silicate−Surfactant Liquid Crystals, *J. Am. Chem. Soc.*, **119**, 3596 **(1997)**

2. Kresge C.T., Leonowicz M.E., Roth W.J., Vartuli J.C. and Beck J.S., Ordered mesoporous molecular sieves synthesized by a liquid-crystal template mechanism, *Nature*, **359**, 710 **(1992)**

3. Corma A., From Microporous to Mesoporous Molecular Sieve Materials and Their Use in Catalysis, *Chem. Rev.*, **97**, 2373 **(1997)**

4. Taguchi A. and Schüth F., Ordered mesoporous materials in catalysis, *Microporous Mesoporous Mater.*, **77(1)**, 1 **(2005)**

5. Bhattacharjee A., Das T., Uyama H., Roy P. and Nandi M., Cu- and Ni-Grafted Functionalized Mesoporous Silica as Active Catalyst for Olefin Oxidation, *Chemistry Select*, **2**, 10157 **(2017)**

6. Ashourirad B., Sekizkardes A.K., Altarawneh S. and El-Kaderi H.M., Exceptional gas adsorption properties by nitrogen-doped porous carbons derived from benzimidazole-linked polymers, *Chem. Mater.*, **27**, 1349 **(2015)**

7. Nandi M., Okada K., Dutta A., Bhaumik A., Maruyama J., Derks D. and Uyama H., Unprecedented $CO_2$ uptake over highly porous N-doped activated carbon monoliths prepared by physical activation, *Chem. Commun.*, **48**, 10283 **(2012)**

8. Coronado E. and Palomares E., Hybrid molecular materials for optoelectronic devices, *J. Mater. Chem.*, **15**, 3593 **(2005)**

9. Das T., Roy A., Uyama H., Roy P. and Nandi M., 2-Hydroxy-naphthyl functionalized mesoporous silica for fluorescence sensing and removal of aluminum ion, *Dalton Trans.*, **46**, 7317 **(2017)**

10. Okada K., Nandi M., Maruyama J., Oka T., Tsujimoto T., Kondoh K. and Uyama H., Fabrication of mesoporous polymer monolith: a template-free approach, *Chem. Commun.*, **47**, 7422 **(2011)**

11. Deng Y.H., Yu T., Wan Y., Shi Y.F., Meng Y., Gu D., Zhang L.J., Huang Y., Liu C., Wu X.J. and Zhao D.Y., Ordered Mesoporous Silicas and Carbons with Large Accessible Pores Templated from Amphiphilic Diblock Copolymer Poly (ethylene oxide)-b-polystyrene, *J. Am. Chem. Soc.*, **129**, 1690 **(2007)**

12. Kosonen H., Valkama S., Nykanen A., Toivanen M., Brinke G. ten, Ruokolainen J. and Ikkala O., Functional porous structures based on the pyrolysis of cured templates of block copolymer and phenolic resin, *Adv. Mater.*, **18**, 201 **(2006)**

13. Nandi M., Gangopadhyay R. and Bhaumik A., Mesoporous polyaniline having high conductivity at room temperature, *Microporous Mesoporous Mater.*, **109**, 239 **(2008)**

14. Meng Y., Gu D., Zhang F.Q., Shi Y.F., Yang H.F., Li Z., Yu C.Z., Tu B. and Zhao D.Y., Ordered mesoporous polymers and

homologous carbon frameworks: amphiphilic surfactant templating and direct transformation, *Angew. Chem. Int. Ed.*, **44**, 7053 **(2005)**

15. Meng Y., Gu D., Zhang F.Q., Shi Y.F., Cheng L., Feng D., Wu Z.X., Chen Z.X., Wan Y., Stein A. and Zhao D.Y., A family of highly ordered mesoporous polymer resin and carbon structures from organic− organic self-assembly, *Chem. Mater.*, **18**, 4447 **(2006)**

16. Nandi M. and Bhaumik A., Nanorods of all organic porous m-cresol–formaldehyde having photoluminescence at room temperature, *Mater. Chem. Phys.*, **114**, 785 **(2009)**

17. Wan Y., Shi Y.F. and Zhao D.Y., Designed synthesis of mesoporous solids via nonionic-surfactant-templating approach, *Chem. Commun.*, DOI: 10.1039/B610570J, 897 **(2007)**

18. Zhang F., Meng Y., Gu D., Yan Y., Yu C., Tu B. and Zhao D., A facile aqueous route to synthesize highly ordered mesoporous polymers and carbon frameworks with Ia $\bar{3}$ d bicontinuous cubic structure, *J. Am. Chem. Soc.*, **127**, 13508 **(2005)**

19. Jang J. and Bae J., Fabrication of mesoporous polymer using soft template method, *Chem. Commun.*, DOI: 10.1039/B416518G, 1200 **(2005)**

20. Peng H., Ma G., Sun K., Mu J., Zhang Z. and Lei Z., Facile synthesis of poly (p-phenylenediamine)-derived three-dimensional porous nitrogen-doped carbon networks for high performance supercapacitors, *J. Phys. Chem. C*, **118**, 29507 **(2014)**

21. Sakintuna B. and Yurum Y., Templated porous carbons: a review article, *Ind. Eng. Chem. Res.*, **44**, 2893 **(2005)**

22. Anderson M.L., Stroud R.M. and Rolison D.R., Enhancing the activity of fuel-cell reactions by designing three-dimensional nanostructured architectures: catalyst-modified carbon-silica composite aerogels, *Nano Lett.*, **2**, 235 **(2002)**

23. Pierre A.C. and Pajonk G.M., Chemistry of aerogels and their applications, *Chem. Rev.*, **102**, 4243 **(2002)**

24. Dillon A.C., Jones K.M., Bekkedahl T.A., Kiang C.H., Bethune D.S. and Heben M.J., Storage of hydrogen in single-walled carbon nanotubes, *Nature*, **386**, 377 **(1997)**

25. Joo S.H., Choi S.J., Oh I., Kwak J., Liu Z., Terasaki O. and Ryoo R., Ordered nanoporous arrays of carbon supporting high dispersions of platinum nanoparticles, *Nature*, **412**, 169 **(2001)**

26. Zhang L.L. and Zhao X.S., Carbon-based materials as supercapacitor electrodes, *Chem. Soc. Rev.*, **38**, 2520 **(2009)**

27. Lu A.H., Schmidt W., Matoussevitch N., Bonnemann H., Spliethoff B., Tesche B., Bill E., Kiefer W. and Schüth F., Nanoengineering of a magnetically separable hydrogenation catalyst, *Angew. Chem. Int. Ed.*, **43**, 4303 **(2004)**

28. Su F., Zeng J., Bao X., Yu Y., Lee J.Y. and Zhao X.S., Preparation and characterization of highly ordered graphitic mesoporous carbon as a Pt catalyst support for direct methanol fuel cells, *Chem. Mater.*, **17**, 3960 **(2005)**

29. Han B.H. and Zhou W.A., Direct preparation of nanoporous carbon by nanocasting, *J. Am. Chem. Soc.*, **125**, 3444 **(2003)**

30. Kim T.W., Ryoo R., Gierszal K.P., Jaroniec M., Solovyov L.A., Sakamoto Y. and Terasaki O., Characterization of mesoporous carbons synthesized with SBA-16 silica template, *J. Mater. Chem.*, **15**, 1560 **(2005)**

31. Lu A.H., Schmidt W., Taguchi A., Spliethoff B., Tesche B. and Schüth F., Taking Nanocasting One Step Further: Replicating CMK-3 as a Silica Material, *Angew. Chem. Int. Ed.*, **41**, 3489 **(2002)**

32. Yu C.Z., Fan J., Tian B.Z., Zhao D.Y. and Stucky G.D., High-yield synthesis of periodic mesoporous silica rods and their replication to mesoporous carbon rods, *Adv. Mater.*, **14**, 1742 **(2002)**

33. Deng Y., Liu C., Gu D., Yu T., Tu B. and Zhao D., Thick wall mesoporous carbons with a large pore structure templated from a weakly hydrophobic PEO–PMMA diblock copolymer, *J. Mater. Chem.*, **18**, 91 **(2008)**

34. Huang Y., Cai H.Q., Yu T., Zhang F.Q., Zhang F., Meng Y., Gu D., Wan Y., Sun X.L., Tu B. and Zhao D.Y., Formation of Mesoporous Carbon with a Face-Centered-Cubic Fd$_3$m Structure and Bimodal Architectural Pores From the Reverse Amphiphilic Triblock Copolymer PPO-PEO-PPO, *Angew. Chem. Int. Ed.*, **46**, 1089 **(2007)**

35. Liang C. and Dai S., Synthesis of mesoporous carbon materials via enhanced hydrogen-bonding interaction, *J. Am. Chem. Soc.*, **128**, 5316 **(2006)**

36. Liu C., Li L., Song H. and Chen X., Facile synthesis of ordered mesoporous carbons from F108/resorcinol–formaldehyde composites obtained in basic media, *Chem. Commun.*, Doi: 10.1039/B614199D, 757 **(2007)**

37. Tanaka S., Nishiyama N., Egashira Y. and Ueyama K., Synthesis of ordered mesoporous carbons with channel structure from an organic-organic nanocomposite, *Chem. Commun.*, DOI: 10.1039/B501259G, 2125 **(2005)**

38. Zhang F., Meng Y., Gu D., Yan Y., Yu C.Z., Tu B. and Zhao D.Y., An aqueous cooperative assembly route to synthesize ordered mesoporous carbons with controlled structures and morphology, *Chem. Mater.*, **18**, 5279 **(2006)**

39. Zhang F., Gu D., Yu T., Zhang F., Xie S., Zhang L., Deng Y., Wan Y., Tu B. and Zhao D., Mesoporous Carbon Single-Crystals from Organic-Organic Self-Assembly, *J. Am. Chem. Soc.*, **129**, 7746 **(2007)**

40. Xia Y., Yang Z. and Mokaya R., Mesostructured hollow spheres of graphitic N-doped carbon nano cast from spherical mesoporous silica, *J. Phys. Chem. B*, **108**, 19293 **(2004)**

41. Dong H., Prasad S., Nyame V. and Jones Jr. W.E., Sub-micrometer conducting polyaniline tubes prepared from polymer fiber templates, *Chem. Mater.*, **16**, 371 **(2004)**

42. Huang Q. R., Kim H.C., Huang E., Mecerreyes D., Hedrick J.L., Volksen W.C., Frank W. and Miller R.D., Miscibility in Organic/Inorganic Hybrid Nanocomposites Suitable for Microelectronic Applications: Comparison of Modulated Differential Scanning Calorimetry and Fluorescence Spectroscopy, *Macromolecules*, **36**, 7661 **(2003)**

43. Li W.C., Lu A.H. and Guo S.C., Characterization of the microstructures of organic and carbon aerogels based upon mixed cresol–formaldehyde, *Carbon*, **39**, 1989 **(2001)**

44. Roy D., Basu P.K., Raghunathan P. and Eswaran S.V., Designing of high-resolution photoresists: use of modern NMR techniques for evaluating lithographic performance, *Bull. Mater. Sci.*, **27**, 303 **(2004)**

45. Kim T.W. and Solovyov L.A., Synthesis and characterization of large-pore ordered mesoporous carbons using gyroidal silica template, *J. Mater. Chem.*, **16**, 1445 **(2006)**.